View Article Online DOI: 10.1039/D4SC03430A

## **ARTICLE**

# Copper Catalyzed Benzylic sp<sup>3</sup> C-H Alkenylation

Ting-An Chen, a, b Richard J. Staples, b and Timothy H. Warrenb

Received 00th January 20xx, Accepted 00th January 20xx

DOI: 10.1039/x0xx00000x

The prenyl group is present in numerous biologically active small molecule drugs and natural products. We introduce benzylic C-H alkenylation of substrates Ar-CH<sub>3</sub> with alkenylboronic esters (CH<sub>2</sub>)<sub>3</sub>O<sub>2</sub>B-CH=CMe<sub>2</sub> as a pathway to form prenyl functionalized arenes Ar-CH<sub>2</sub>CH=CMe<sub>2</sub>. Mechanistic studies of this radical relay catalytic protocol reveal diverse reactivity pathways exhibited by the copper(II) vinyl intermediate [Cu<sup>II</sup>]-CH=CMe<sub>2</sub> that involve radical capture, bimolecular C-C bond formation, and hydrogen atom transfer (HAT).

#### Introduction

The prenyl group (-CH<sub>2</sub>CH=CMe<sub>2</sub>) is a prevalent functionality found in natural products and biologically active small molecules.<sup>1–6</sup> Prenyltransferase, an essential enzyme involved in prenylation,

a. Prenylated drug molecules

c. Previous sp<sup>3</sup> C-H alkenylation

d. This work: benzylic C-H alkenylation

**Fig. 1.** (a) Prenylated natural products and drug molecules. (b) Prenylation via cross-coupling. (c) sp<sup>3</sup> C-H styrenylation. (d) Net prenylation via benzylic C-H alkenylation.

enhances protein stability and anchors proteins to cell membranes due to the hydrophobic nature of the prenyl group. <sup>7–10</sup> The addition of a prenyl group to molecules can influence their biological activities. <sup>11–14</sup> For instance, the prenyl group is the primary inhibitory component of the HIV inhibitor Osthol (Fig. 1a). <sup>15</sup> Additionally, both experimental and computational methods to determine that prenylated chrysin functions as a more potent inhibitor for P-glycoprotein, a determinant of drug accumulation in leukemia cells. <sup>16,17</sup>

Methods for installing prenyl groups onto aromatic rings typically involve C-C coupling through allylation of an aryl halide (or pseudohalide) (Fig. 1b). For instance, Pd catalyzed Suzuki or Negishi coupling reactions produce prenylated aryl derivatives. 18–20 Alternatively, sp<sup>2</sup> C-H prenylation of arene C-H bonds with 1,1-dimethylallene also leads to aryl prenyl derivatives. 21–24

This report presents an alternative strategy to prenyl-functionalized molecules through C-H alkenylation of benzylic C-H

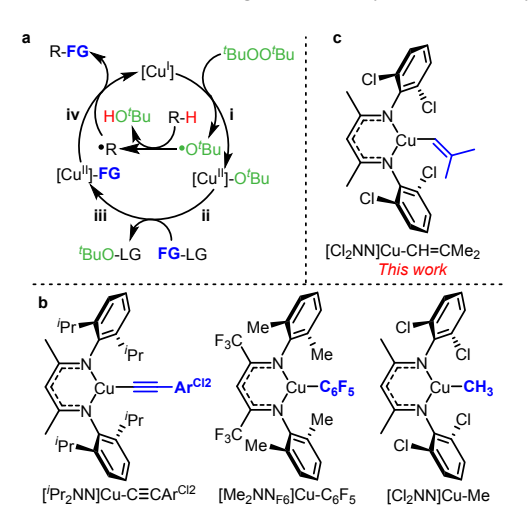


**Fig. 2.** (a) Radical relay mechanism for C-H functionalization. (b)  $\beta$ -diketiminato copper(II) intermediates in C-H alkynylation, arylation and methylation. (c) Proposed copper(II) alkenyl intermediate for C-H alkenylation.

<sup>&</sup>lt;sup>a.</sup> Department of Chemistry, Georgetown University, Washington, D.C. 20057, United States.

b. Department of Chemistry, Michigan State University, East Lansing, Michigan 48824, United States.

c-†Electronic Supplementary Information (ESI) available: [details of any supplementary information available should be included here]. See DOI: 10.1039/x0xx00000x

scepted Manu

ARTICLE Journal Name

bonds via the alkenylboronic ester (CH<sub>2</sub>)<sub>3</sub>O<sub>2</sub>B-CH=CMe<sub>2</sub> (Fig. 1d). Previous examples of direct sp<sup>3</sup> C-H alkenylation with alkenylboronic esters required highly acidic C-H bonds in aryl difluoromethyl derivatives Ar-CF<sub>2</sub>H.<sup>25</sup> Alternatively, benzylic sp<sup>3</sup> C-H styrenylation occurs with styrenyl carboxylates and nitrites in the presence of  $^tBuOO^tBu$  (Fig. 1c). $^{26-30}$ 

This report utilizes the dimethylethenyl (-CH=CMe<sub>2</sub>) group as the alkene source for sp³ C-H functionalization. Our research team and other groups have employed radical relay approaches for C-H functionalization (Fig. 2a).  $^{31-35}$  Based on sp³ C-H alkynylation,  $^{36}$  arylation,  $^{37,38}$  and methylation  $^{39}$  that proceed via [Cu<sup>II</sup>]-C  $\equiv$  CAr, [Cu<sup>II</sup>]-Ar, and [Cu<sup>II</sup>]-Me intermediates, respectively (Fig. 2b), we anticipated that [Cu<sup>II</sup>]-CH=CMe<sub>2</sub> intermediates (Fig. 2c) could lead to benzylic sp³ C-H alkenylation. This would convert an Ar-CH<sub>2</sub>-H group to Ar-CH<sub>2</sub>-CH=CMe<sub>2</sub>, enabling net prenylation (Fig. 1d).

#### **Results and Discussion**

#### Reaction Discovery and Optimization.

We sought to enable benzylic C-H alkenylation, employing toluene as a representative benzylic substrate using Cu(I) β-diketiminato complexes as catalysts along with di-*tert*-butyl peroxide ('BuOO'Bu) as the oxidant. We chose alkenylboronic esters as the alkenyl source but recognized that the nature of the boronic ester backbone could play an important role (Scheme 1). For example, 4,4,6-trimethyl-2-phenyl-1,3,2-dioxaborinane exhibited a higher yield in sp³ C-H arylation compared to phenylboronic acid pinacol ester.<sup>38</sup> Therefore, we investigated 2-alkenyl-1,3,2-dioxaborinane (2a) and 4,4,6-trimethyl-2-alkenyl-1,3,2-dioxaborinane (2b) as possible alkenyl group transfer reagents for C-H alkenylation of

**Scheme 1.** Steric effect of the alkene source to alkenylation yield. **Table 1.** Catalyst optimization for C-H alkenylation.

Conditions: 20 equiv. of R-H, 2 equiv. <sup>t</sup>BuOO<sup>t</sup>Bu, 60 °C, 1 h. Yields are determined by GCMS analysis.

toluene (Scheme 1). Use of the less sterically hindered, boronic ester 2a produced a higher C-H alkenylation yield of produce 3a that with the more sterically hindered boronic ester 2b (63% vs. 15%, respectively). Importantly, the more hindered boronic ester 2b led to toluene C-H etherification to give PhCH<sub>2</sub>-O'Bu that signals capture of the benzyl radical PhCH<sub>2</sub>• by the [Cu<sup>II</sup>]-O'Bu intermediate (Scheme S1). 40 We hypothesize that a higher rate of transmetalation between the [Cu<sup>II</sup>]-O'Bu intermediate and the less sterically hindered alkenylboronic ester 2a to form a [Cu<sup>II</sup>]-C=CMe<sub>2</sub> intermediate inhibits the formation of PhCH<sub>2</sub>O'Bu (Scheme S1).

Employing boronic ester **2a**, we explored various parameters including the solvent, catalyst loading (Table S1), oxidant (Table S2), temperature (Table S4). Using optimized conditions (10 mol% [Cu¹], 2 equiv.  $^tBuOO^tBu$ , 20 equiv. R-H, 300  $\mu L$  benzene, and 60 °C), we also examined different copper  $\beta$ -diketiminate catalysts with diverse electronic and steric properties (Table 1). Among the tested catalysts, [Cl₂NN]Cu (Table 1, entry 1) gave the highest product yield. Interestingly, a very electron-poor catalyst (Table 1, entry 2) gave a very low yield, yet catalysts with electron-donating groups on the  $\beta$ -diketiminato N-aryl rings also decreased the product yield.

#### Benzylic C-H Alkenylation Leading to Net Prenylation

We systematically examined a range of benzylic R-H substrates, assessing reaction yields via GCMS analysis (Table 2). We initially

Table 2. Cu catalysed C-H alkenylation.

Detail reaction condition is in supporting information. Yields are determined by GCMS <sup>†</sup>80 °C. \*100 °C. \*10 eq of R-H substrate was used. Isolated yield in parenthesis.

**Journal Name ARTICLE** 

focused on sp<sup>3</sup> C-H alkenylation of commercially available benzylic substrates Ar-CH3 that lead to prenyl derivatives ArCH2-CH=CMe2 (3a-3i) in 42-92% yield. Slightly higher yields result in more electronrich substrates Ar-CH<sub>3</sub> (3b, 3d, 3e; 64-92%). This method tolerates aryl halides Ar-X (3f - 3h) that typically serve as substrates in more traditional cross-coupling reactions. The method also tolerates ortho-substitution as illustrated by the use of o-chlorotoluene and oxylene (3i and 3j) for C-H alkenylation. Secondary benzylic C-H sites in ethylbenzene also undergo C-H alkenylation (31), yet exhibit lower yields due to the formation of styrene in 20% yield via  $\beta$ -H-atom abstraction from the ethylbenzene radical (PhCH(•)Me) (Supporting Information, Section 4 and Scheme S5). Additionally, N,N-dimethyl aniline (30) proved amenable to  $\alpha$ -N C-H functionalization, albeit in lower yield (22 %). We also examined indoles with heteroaryl-Me groups, but unfortunately no C-H alkenylation occurs, even with N-Boc protected indoles.

To highlight potential advantages of prenylation via benzylic C-H alkenylation, we performed C-H alkenylation on three pharmaceutically relevant compounds (3p - 3r). Notably, our method exhibited high selectivity for benzylic C-H bonds. For example, in the case of nabumetone (3p) which possesses multiple sp<sup>3</sup> C-H bonds, exclusive benzylic C-H functionalization occurs. Entry 3r yielded a product closely related to its o-OMe derivative with HIV inhibitory properties, highlighting the potential of this direct C-H alkenylation method to condense lengthy syntheses.<sup>15</sup> Yet we recognize the rather modest yields for the C-H functionalization step with these compounds (Table 2, entries 3p - 3r); some substrates lead to relatively strong binding with the [Cu<sup>1</sup>] catalyst that impedes C-H functionalization (Scheme S2; Fig. S4).

#### **Mechanistic Investigations**

To gain more insight into the interaction between the alkenylboronic ester and the [Cu1] catalyst as well as the formation and reactivity of the proposed [Cu<sup>II</sup>]-CH=CMe<sub>2</sub> intermediate, we examined facets of the reaction mechanism by integrating both

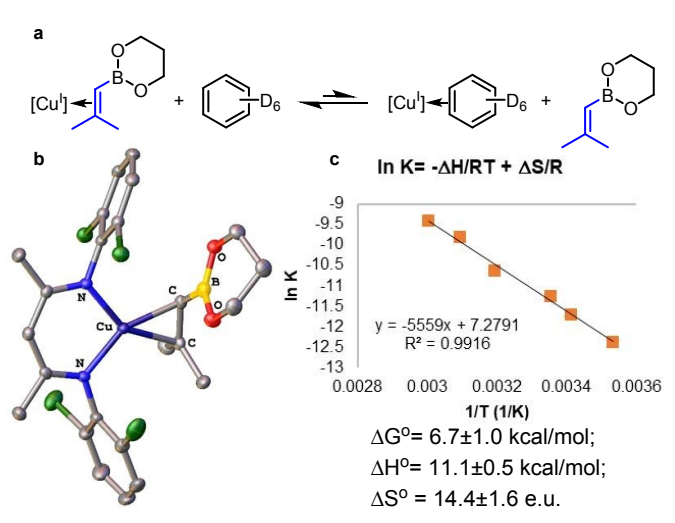


Fig. 3. (a) reversible binding of 2a to [Cu<sup>1</sup>] catalyst in benzene, (b) Xray structure of alkenylboronic ester adduct, and (c) van't Hoff plot.

experimental and computational analyses.

View Article Online

Alkenylboronic ester binding to copper(I) catalyst.1039/D4SC03430A

Given the need for mild heating to encourage C-H alkenylation, we considered the possibility of equilibrium binding of the dimethylethenylboronic ester 2a with the [Cu<sup>1</sup>] catalyst (Fig. 3a). The crystal structure of the  $[Cu^{I}](\eta^{2}$ -2a) adduct reveals an interaction between the  $\pi$  electrons of the alkene and the [Cu<sup>I</sup>] catalyst (Fig. 3b). Higher temperatures promote the dissociation of this adduct, leading to increased concentrations of the dissociated species. A van't Hoff plot reveals thermodynamic parameters corresponding to this equilibrium:  $\Delta G_{exp}(298) = 6.7 \pm 1.0$ ,  $\Delta H_{exp} = 11.1 \pm 0.5$  kcal/mol, and  $\Delta S_{exp}$ = 14.4 ± 1.6 e.u. (Figs. 3c and S2).

#### Formation and Reactivity of Alkenyl Intermediate [Cu<sup>II</sup>]-C=CMe<sub>2</sub>.

Mixing [Cu<sup>II</sup>]-O<sup>t</sup>Bu with **2a** in fluorobenzene produces a substantial amount of 2,5-dimethylhexa-2,4-diene (alkenyl dimer) (84% yield, Fig. 4a). This could proceed via a [Cu<sup>II</sup>]-CH=CMe2 intermediate that undergoes bimolecular C-C coupling to give the observed alkenyl dimer, much as  $[Cu^{II}]-C \equiv$ CAr and  $[Cu^{II}]$ -Ar intermediates readily form ArC  $\equiv$  C-C  $\equiv$  CAr<sup>36</sup> and Ar-Ar<sup>37</sup> species. In situ UV-vis analysis was employed to monitor the reaction intermediate of [Cu<sup>II</sup>]-O<sup>t</sup>Bu and **2a** (Fig. S6). Upon introducing 2a into the [Cu<sup>II</sup>]-O<sup>t</sup>Bu solution at -38 °C, a rapid reaction occurred, leading to a decrease in the absorption band of [Cu<sup>II</sup>]-O<sup>t</sup>Bu without the detection of any newly generated [Cull] species. Based on previous bimolecular C-C bond formation via [Cu<sup>II</sup>]-C=CAr<sup>36</sup> and [Cu<sup>II</sup>]-Ar<sup>37</sup> species, we propose that the [Cu<sup>II</sup>]-CH=CMe<sub>2</sub> intermediate similarly undergoes rapid bimolecular C-C coupling to form Me<sub>2</sub>C=CH-CH=CMe2. Indeed, it is possible for a conjugated diene to bridge between two  $\beta$ -diketiminato [Cu<sup>1</sup>] to form a [Cu<sup>1</sup>]<sub>2</sub>( $\mu$ -diene) species (Fig. S8).

Fig. 4. Reaction of [Cl<sub>2</sub>NN]Cu-O<sup>t</sup>Bu and 2a (a) in C<sub>6</sub>H<sub>5</sub>F, (b) in the presence of Gomberg's dimer in C<sub>6</sub>H<sub>5</sub>F, and (c) in toluene. †isolated yield.

To further confirm the reaction intermediate obtained upon addition of alkenylboronic ester 2a with [Cu<sup>II</sup>]-O<sup>t</sup>Bu as [Cu<sup>II</sup>]-CH=CMe<sub>2</sub>, reaction in the presence of Gomberg's dimer (that dissociates to produce the trityl radical Ph<sub>3</sub>C•) provides Ph<sub>3</sub>C-CH=Me<sub>2</sub> in 35% yield (Fig. 4b). Additionally, a minimal amount of 3a also forms when the reaction occurs in toluene

ARTICLE Journal Name

(Fig. 4c). Product **3a** can arise from the sequential steps of toluene radical formation through HAT, followed by subsequent radical capture (Fig. 5c).

#### Computational analysis and insights.

We employed density functional theory (DFT) to better understand and interpret the above experimental findings. Remarkably, the experimental thermodynamic parameters derived from the van't Hoff plot for the binding of the alkenylboronic ester to [Cu¹], closely correspond to the predictions from density functional theory (DFT), with  $\Delta G_{DFT}=7.5~kcal/mol$ ,  $\Delta H_{DFT}=11.5~kcal/mol$ , and  $\Delta S_{DFT}=12.1~e.u.$  (Fig. 5a). The strong agreement between experimental data ( $\Delta G_{exp}=6.7\pm1.0~kcal/mol$ ) and DFT results supports the reliability of the thermodynamic data from calculations. Furthermore, the alkenylated product  $\bf 3a$  exhibits a lower affinity for binding to

$$[Cu^l] + C_6H_6 \xrightarrow{\Delta G = 7.5} [Cu^l](\eta^2 - C_6H_6) + BO$$

$$[Cu^l] + C_6H_6 \xrightarrow{\Delta G = 5.9} [Cu^l](\eta^2 - C_6H_6) + BO$$

$$Cu: 0.42 \qquad Contour value: 0.01$$

$$Cu: 0.42 \qquad Contour value: 0.01$$

$$Cl \qquad ii. Ph_3C \xrightarrow{Radical} [Cu^l] \qquad Ph$$

$$\Delta G = -69.1 \qquad [Cu^l] \qquad Ph$$

$$\Delta G = -39.0 \qquad Cu^l \rightarrow Ph$$

$$\Delta G = -61.8 \qquad Capture$$

**Fig. 5.** DFT calculation of (a)  $[Cu^{I}]$  binds to alkenes, **2a** and **3a**. (b) spin density plot of  $[Cu^{II}]$ -CH=CMe<sub>2</sub>. (c) possible reaction pathways for  $[Cu^{II}]$ -CH=CMe<sub>2</sub>. Free energies in kcal/mol at 298.15 K. For more details, see Schemes S3 and S4.

 $\Delta G = -8.2$  $\Delta G^{\ddagger} = 12.9$  [Cu<sup>I</sup>] compared to **2a** (ΔG<sub>DFT</sub> = 5.9 kcal/mol) (Scheme S4) cle Online

This result is consistent with the need of the large (60°C) to disrupt the interaction between alkenyl precursors or products  $\bf 2a$  or  $\bf 3a$  and the [Cu<sup>I</sup>] catalyst, thereby initiating the catalytic cycle. Upon dissociation of the alkene from the [Cu<sup>I</sup>] catalyst, the [Cu<sup>I</sup>] complex undergoes oxidation by 'BuOO'Bu which requires on an accessible coordination site. <sup>40</sup> Furthermore, the formation of [Cu<sup>II</sup>]-CH=CMe<sub>2</sub> via transmetalation of [Cu<sup>II</sup>]-O'Bu with  $\bf 2a$  is exergonic ( $\Delta G = -3.5$  kcal/mol) with a modest reaction barrier ( $\Delta G^{\ddagger} = 13.6$  kcal/mol) (Scheme S3).

A spin density plot of the  $[\text{Cu}^{\text{II}}]\text{-CH=CMe}_2$  intermediate indicates 31% localization on  $C_\alpha$  (Fig. 5b). The radical nature of the alkenyl group bound to the copper(II) center in  $[\text{Cu}^{\text{II}}]\text{-CH=CMe}_2$  also accounts for its propensity to dimerize to form  $\text{Me}_2\text{C=CH-CH=CMe}_2$ , a highly favorable reaction  $(\Delta G_{\text{rxn}} = -69.1 \text{ kcal/mol})$ . A relaxed energy scan for dimerization further reveals essentially no barrier for this process (Fig. S22). Similarly, the radical capture by trityl radical pathway is also a highly favourable reaction ( $\Delta G = -39.0 \text{ kcal/mol}$ ) (Fig. 5c ii). We note that loss of the alkenyl radical  $\bullet \text{CH=CMe}_2$  from [Cu<sup>II</sup>]-CH=Me $_2$  is significantly uphill in free energy ( $\Delta G = 36.0 \text{ kcal/mol}$ ; Figure S21); accordingly we do not anticipate the direct involvement of the  $\bullet \text{CH=CMe}_2$  radical in these copper-catalyzed reactions.

Due to the radical character on  $C_{\alpha}$ , we investigated whether  $[Cu^{\shortparallel}]$ -CH=CMe $_2$  could abstract a H-atom from a benzylic C-H bond. This HAT process is favourable with a relatively low reaction barrier ( $\Delta G$ = -8.2 kcal/mol;  $\Delta G$ \*= 12.9 kcal/mol; Fig. 5c iv). This calculation result is consistent with the experiment, where a trace amount of alkenylation product, **3a**, was observed in the absence of  $^tBuO$ • (Fig. 4c). After  $[Cu^{\shortparallel}]$ -CH=CMe $_2$  abstracts an H atom from toluene, the resulting toluene radical undergoes capture by  $[Cu^{\shortparallel}]$ -CH=CMe $_2$  to form **3a** (Fig. 5c iii). Calculations also rationalize the formation of styrene as a byproduct in the C-H alkenylation of ethylbenzene. Both radical capture and H-atom abstraction of a  $\beta$ -H of the 2° ethylbenzene radical PhCH(•)Me are extremely favorable ( $\Delta G$  = -55.0 and -48.3 kcal/mol, respectively; Scheme S5)

### **Conclusions**

This report illustrates the use of alkenylboronic esters in catalytic benzylic C-H functionalization for  $sp^3\text{-}sp^2$  C-C bond construction. The  $Me_2C$ =CH-B(OR) $_2$  reagent 2a exhibits a broad C-H substrate scope across typical 1° benzylic C-H bonds. Importantly, it significantly expands the scope for benzylic C-H alkenylation as it does not require highly acidified ArCF $_2$ -H bonds.  $^{25}$  Importantly, this study illustrates how  $sp^3$  C-H alkenylation can lead to formation of the prenyl group known to engender biological activity in small molecules.

A combination of experimental and computational studies support that this sp³ C-H alkenylation protocol proceeds via a copper(II) alkenyl intermediate [Cu $^{\text{II}}$ ]-CH=CMe $_2$  (Scheme 2). This [Cu $^{\text{II}}$ ]-CH=CMe $_2$  intermediate promotes C-C bond formation to form R-CH=CMe $_2$  products in the capture of an alkyl radical R•

**Journal Name ARTICLE** 

Scheme 2. Catalytic cycle for sp<sup>3</sup> C-H alkenylation with competing pathways via the [Cu<sup>II</sup>]-CH=CMe<sub>2</sub> intermediate.

derived from H-atom abstraction from R-H via the <sup>t</sup>BuO • radical generated upon reaction of 'BuOO'Bu with [Cul]. Facile bimolecular C-C coupling between [Cu<sup>II</sup>]-CH=CMe<sub>2</sub> species results in a competing pathway to form the diene Me<sub>2</sub>C=CH-CH=CMe2. Yet, the copper(II) alkenyl intermediate can also directly transform substrates R-H into R-CH=CMe2, albeit in low yield, due to the ability of the [Cu<sup>II</sup>]-CH=CMe<sub>2</sub> intermediate to abstract a H-atom from substrates R-H to form R. This unusual chemical pathway available uncovered for copper(II) alkenyls offers additional opportunities to construct catalytic C-H alkenylation protocols via selective H-atom abstraction of substrates R-H via metal-centred intermediates en route to functionalized species R-CH=CRR'.

### **Experimental section**

Detailed experimental procedures are provided in the ESI.<sup>†</sup>

### Data availability

All synthetic procedures, characterization data, spectroscopic data, computational data, supplementary figures and tables, and detailed crystallographic information can be found in the ESI.<sup>†</sup> available Crystallographic data are via the Crystallographic Data Centre (CCDC): 2268882 and 2329536.

### **Author Contributions**

T.-A.C. and T.H.W. conceived project. T.-A.C. carried out experimental and computational works. T.-A.C. and R.J.S. collected, solved, and refined crystallographic data. T.H.W. supervised the experimental and computational work. T.-A.C. and T.H.W. wrote the manuscript. All authors have given approval to the final version of the manuscript.

#### **Conflicts of interest**

There are no conflicts to declare.

### Acknowledgements

DOI: 10.1039/D4SC03430A We are grateful to NSF (CHE-1955942 and CHE-2303206) for

View Article Online

supporting this work. The Rigaku Synergy S Diffractometer was purchased with support of the NSF MRI program (CHE-1919565). We extend our gratitude to Dr. Joseph Gair for assisting us with the development of a chemical space diagram, Dr. Daniel Holmes for help in variable temperature NMR experiments, and Dr. Anthony Schilmiller for insightful discussions regarding HRMS analyses.

#### Notes and references

- 1 M. E. G. Mosquera, G. Jiménez, V. Tabernero, J. Vinueza-Vaca, C. García-Estrada, K. Kosalková, A. Sola-Landa, B. Monje, C. Acosta, R. Alonso and M. Á. Valera, Sustain. Chem., 2021, 2, 467–492.
- J. D. Ochocki and M. D. Distefano, Med. Chem. Commun., 2013, **4**, 476-492.
- 3 K. Šmejkal, *Phytochem Rev*, 2014, **13**, 245–275.
- M. E. Tanner, Nat. Prod. Rep., 2014, 32, 88-101.
- X. Yang, Y. Jiang, J. Yang, J. He, J. Sun, F. Chen, M. Zhang and B. Yang, Trends Food Sci., 2015, 44, 93-104.
- R. Ciochina and R. B. Grossman, Chem. Rev., 2006, 106, 3963-3986.
- P.-H. Liang, T.-P. Ko and A. H.-J. Wang, Eur. J. Biochem., 2002, **269**, 3339-3354.
- 8 D. P. Labbé, S. Hardy and M. L. Tremblay, Prog Mol Biol Transl *Sci*, 2012, **106**, 253–306.
- C. C. Palsuledesai and M. D. Distefano, ACS Chem. Biol., 2015,
- 10 E. S. Marakasova, N. K. Akhmatova, M. Amaya, B. Eisenhaber, F. Eisenhaber, M. L. van Hoek and A. V. Baranova, Mol Biol, 2013,
- 11 B. Botta, A. Vitali, P. Menendez, D. Misiti and G. D. Monache, Curr. Med. Chem., 2005, 12, 713-739.
- 12 M. M. M. Pinto, M. E. Sousa and M. S. J. Nascimento, Curr. Med. Chem., 12, 2517-2538.
- 13 K. Yazaki, K. Sasaki and Y. Tsurumaru, Phytochem., 2009, 70, 1739-1745.
- 14 X. Chen, E. Mukwaya, M.-S. Wong and Y. Zhang, Pharm Biol, 2014, **52**, 655-660.
- 15 S. Tamura, T. Fujitani, M. Kaneko and N. Murakami, Bioorg. Med. Chem. Lett., 2010, 20, 3717-3720.
- 16 G. Comte, J.-B. Daskiewicz, C. Bayet, G. Conseil, A. Viornery-Vanier, C. Dumontet, A. Di Pietro and D. Barron, J. Med. Chem., 2001, 44, 763-768.
- 17 R. Badhan and J. Penny, Eur. J. Med. Chem., 2006, 41, 285-295.
- 18 Y. Yang and S. L. Buchwald, J. Am. Chem. Soc., 2013, 135, 10642-10645.
- 19 Y. Yang, T. J. L. Mustard, P. H.-Y. Cheong and S. L. Buchwald, Angew. Chem. Int. Ed., 2013, **52**, 14098–14102.
- 20 J. L. Farmer, H. N. Hunter and M. G. Organ, J. Am. Chem. Soc., 2012, 134, 17470-17473.
- 21 M. A. Tarselli, A. Liu and M. R. Gagné, Tetrahedron, 2009, 65,
- 22 Y. J. Zhang, E. Skucas and M. J. Krische, Org. Lett., 2009, 11, 4248-4250.

**Shemical Science Accepted Manuscript** 

View Article Online DOI: 10.1039/D4SC03430A

**ARTICLE Journal Name** 

23 S.-Y. Chen, Q. Li and H. Wang, J. Org. Chem., 2017, 82, 11173-

- 24 R. Zeng, C. Fu and S. Ma, J. Am. Chem. Soc., 2012, 134, 9597-9600.
- 25 K. Chakrabarti, M. M. W. Wolfe, S. Guo, J. W. Tucker, J. Lee and N. K. Szymczak, Chem. Sci., 2024, 15, 1752-1757.
- 26 S. Guo, Y. Yuan and J. Xiang, New J. Chem., 2015, 39, 3093-
- 27 Z. Fang, C. Wei, J. Lin, Z. Liu, W. Wang, C. Xu, X. Wang and Y. Wang, Org. Biomol. Chem., 2017, 15, 9974-9978.
- 28 Z. Cui, X. Shang, X.-F. Shao and Z.-Q. Liu, Chem. Sci., 2012, 3,
- 29 H. Yang, P. Sun, Y. Zhu, H. Yan, L. Lu, X. Qu, T. Li and J. Mao, Chem. Commun., 2012, 48, 7847-7849.
- 30 H. Yang, H. Yan, P. Sun, Y. Zhu, L. Lu, D. Liu, G. Rong and J. Mao, Green Chem., 2013, 15, 976-981.
- 31 D. L. Golden, S.-E. Suh and S. S. Stahl, Nat Rev Chem, 2022, 6, 405-427.
- 32 E. S. Jang, C. L. McMullin, M. Käß, K. Meyer, T. R. Cundari and T. H. Warren, J. Am. Chem. Soc., 2014, 136, 10930-10940.
- 33 M. S. Kharasch and G. Sosnovsky, J. Am. Chem. Soc., 1958, 80, 756-756.
- 34 M. S. Kharasch, G. Sosnovsky and N. C. Yang, J. Am. Chem. Soc., 1959, 81, 5819-5824.
- 35 D. J. Rawlinson and G. Sosnovsky, Synthesis, 1972, 1972, 1–28.
- 36 A. Bakhoda, O. E. Okoromoba, C. Greene, M. R. Boroujeni, J. A. Bertke and T. H. Warren, J. Am. Chem. Soc., 2020, 142, 18483-18490.
- 37 S. Kundu, C. Greene, K. D. Williams, T. K. Salvador, J. A. Bertke, T. R. Cundari and T. H. Warren, J. Am. Chem. Soc., 2017, 139, 9112-9115.
- 38 A. Vasilopoulos, S. L. Zultanski and S. S. Stahl, J. Am. Chem. Soc., 2017, 139, 7705-7708.
- 39 B. C. Figula, T.-A. Chen, J. A. Bertke and T. H. Warren, ACS Catal., 2022, 12, 11854-11859.
- 40 R. T. I. Gephart, C. L. McMullin, N. G. Sapiezynski, E. S. Jang, M. J. B. Aguila, T. R. Cundari and T. H. Warren, J. Am. Chem. Soc., 2012, **134**, 17350-17353.

This article is licensed under a Creative Commons Attribution-NonCommercial 3.0 Unported Licence.

Open Access Article. Published on 19 September 2024. Downloaded on 9/19/2024 8:35:52 AM.

All synthetic procedures, characterization data, spectroscopic data, computational data, supplementary figures and tables, and detailed crystallographic information can be found in the ESI.<sup>†</sup> Crystallographic data are available via the Cambridge Crystallographic Data Centre (CCDC): 2268882 and 2329536.